Improving Safety and Reliability on High-Voltage Lines With Broken Conductor Detection, a Utility's Perspective

Joe Livingston
Great River Energy

Stephen Marx
Bonneville Power Administration

Josh LaBlanc, Yanfeng Gong, Jordan Bell, and Kanchanrao Dase
Schweitzer Engineering Laboratories, Inc.

Presented at the
61st Annual Minnesota Power Systems Conference
Saint Paul, Minnesota
November 4–6, 2025

Originally presented at the
52nd Annual Western Protective Relay Conference, October 2025

Improving Safety and Reliability on High-Voltage Lines With Broken Conductor Detection, a Utility's Perspective

Joe Livingston, *Great River Energy*
Stephen Marx, *Bonneville Power Administration*
Josh LaBlanc, Yanfeng Gong, Jordan Bell, and Kanchanrao Dase, *Schweitzer Engineering Laboratories, Inc.*

***Abstract*—This paper provides real-world examples to demonstrate how broken conductor detection can complement and improve traditional shunt fault protection schemes. Three particular real-world events are analyzed—two from the Great River Energy system and one from the Bonneville Power Administration system. Each event started with a broken conductor and evolved to include a line-to-ground shunt fault on one side of the conductor break. One event resulted in a breaker failure operation caused by a slow breaker, which led to a more impactful outage. In all three events, the shunt faults introduced concerns with ground protection sensitivity—specifically, regarding the ability to detect the shunt fault from the terminal on the opposite side of the break away from the shunted fault. Complementing the existing shunt fault protection schemes with broken conductor detection would have mitigated several concerns in these events.**

A conductor break starts as a series fault before, in many cases, evolving to include a line-to-ground shunt fault on one or both sides of the break. The series fault duration is almost always long enough to measure waveform characteristics of a series fault event, even in a falling conductor scenario. Detecting and isolating the broken conductor in the series fault state results in a safer power system with improved reliability by minimizing the risk of wildfire, the stress on equipment, and the impacts of outages. This paper presents an enhanced broken conductor detection method and, through event analysis, demonstrates its response to the broken conductor events. In addition, the provided discussion demonstrates the benefits of applying broken conductor detection and traditional shunt fault protection concurrently to shore up dependability gaps in traditional detection.

I. Introduction

A broken conductor is a series fault condition resulting from a break in the conductor of a utility transmission or distribution line. Often a broken conductor evolves into a shunt fault condition within the first few seconds of the initial break. Therefore, the series fault condition is easy to overlook in the review of a power system event. This suggests that broken conductor conditions might be a more frequent occurrence than utility protection departments realize. Although series faults place little to no additional stress on the transmission lines and transformers in the power system, they affect loading conditions and impose severe stress on rotating machines. Therefore, it is advantageous to detect and isolate a line during the series fault condition prior to it evolving to include a shunt fault that stresses equipment in the power system and introduces wildfire and public safety risks.

Broken conductors can be difficult to detect, and conductor break events require specialized protection algorithms for successful detection. Much of the focus of broken conductor detection (BCD) in the utility industry today relates to wildfire mitigation strategies. BCD, however, provides benefits to utilities' protection strategies beyond wildfire mitigation. Detecting and isolating broken conductors also enhances power system safety, protects the health of equipment in the power system, and improves relay protection schemes.

Conductor breaks can challenge the sensitivity and dependability of traditional shunt fault protection schemes when the event evolves to include a shunt fault. During these conditions, BCD schemes work well to complement shunt fault protection by isolating the broken conductor before it evolves to include a shunt fault. Later in this paper, we use events from the Great River Energy (GRE) and Bonneville Power Administration (BPA) systems to demonstrate how applying BCD to complement shunt fault protection schemes improves the overall system response during events such as the loss of communications channel or a slow breaker, or when transmission line applications terminate directly into a transformer.

The power system configuration is paramount to the type of BCD required to successfully detect broken conductors. The events presented in this paper occurred on looped transmission systems and, therefore, the BCD analysis within this paper introduces an enhanced algorithm pairing line-charging current [1] and Kirchhoff's current law (KCL) [2] BCD methods for improved BCD performance, which is further explained in Section II. Together, these detection techniques detect conductor breaks with local measurements only, blocking reclosing attempts and locating the conductor break location.

Additional BCD methods suitable for looped transmission and subtransmission systems include detecting the series arcing resulting from a conductor break event [3] and impedance-based methods [4]. The series arcing technique monitors for signatures of series arcing, such as a decrease in current or an increase in phase resistance. This series arcing technique does not provide great selectivity and is best used to enhance the security of other BCD methods or to block reclosing when arcing is detected just prior to a shunt fault relay operation, which is indicative of a broken conductor-caused fault. Impedance-based methods require communications capable of

sharing analog quantities and, therefore, are more complex and more costly to apply. Additionally, impedance-based methods are difficult to set with proper sensitivity to detect a conductor break in the center of a line with significant charging current.

Voltage-based methods can also be deployed on radial transmission and subtransmission lines [5] [6], and require a substantial change in either phase, negative-sequence, or zero-sequence voltage on one side of a conductor break. Therefore, these methods are dependability-challenged in detecting breaks on power lines with multiple sources and require communications capable of sharing analog quantities.

II. Enhanced BCD Algorithm

The charging current-based method for detecting broken conductors relies on the sole presence of line-charging current, which is primarily due to the shunt capacitance of the subtransmission or transmission line. In this approach, the protective relay monitors the phase angle of the line current. Specifically, it looks for a current that leads the corresponding phase voltage by approximately 90 degrees, which is characteristic of capacitive charging current [1]. This angle check requires that the conductor break is forward of the relay location. Additionally, charging current reach settings require that the measured charging current is less than the expected charging current at the element reach, which provides the element with a well-defined reach. The charging current method offers two elements: an underreaching instantaneous element and a time-coordinated element set to overreach the protected line to provide BCD to the end of the line. This method also uses the measured charging current during the conductor break to report the location of the break on the power line.

However, because this method depends on accurately measuring the current angle, it requires a minimum threshold of current magnitude to ensure a reliable angle calculation. If the current is too low, the angle measurement becomes unreliable. This minimum charging current magnitude is 0.7 percent of the relay nominal current input rating and is represented as I_{CH_CC} in Fig. 1 [7]. This limitation makes the charging current method ineffective for detecting a break near the relay terminal or the segment of the line between the relay and the break is too short to produce a significant charging current.

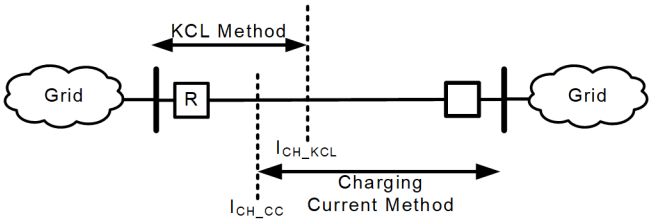

I_{CH_CC} is the minimum and reliable post-conductor-break charging current magnitude to rely on the current angle.

I_{CH_KCL} is the maximum charging current within which KCL method is permitted to operate.

Fig. 1 BCD dependability reach using charging current and KCL methods for a two-terminal power line as implemented in [7].

To address this limitation, the KCL-based method is applied to detect conductor breaks near the relay terminal. The KCL approach evaluates the ratio of the sum of negative- and zero-sequence currents to the compensated positive-sequence current at the relay terminal. For a broken conductor condition, this ratio should be close to –1. The line-charging current compensation in the positive-sequence network can influence the value of this ratio for a broken conductor condition, especially when the charging current from the relay to the broken conductor location is comparable to the line loading on the healthy phases. Reference [2] describes a method for compensating the charging current to achieve a ratio of value –1 for all broken conductor conditions, represented by (1) and the green dot in Fig. 2. This ratio (r) is evaluated in the complex plane against a rectangular operating region with boundaries of –0.9 and –1.1 on the real axis, and 0.05 and –0.05 on the imaginary axis, as represented by the red rectangle in Fig. 2.

$$r = \frac{I_{2L} + I_{0L}}{I_{1L} - I_{1mCH}} \approx -1 \quad (1)$$

where:

I_{2L} is the measured negative-sequence current

I_{0L} is the measured zero-sequence current

I_{1L} is the measured positive-sequence current

I_{1mCH} is the calculated positive-sequence charging current

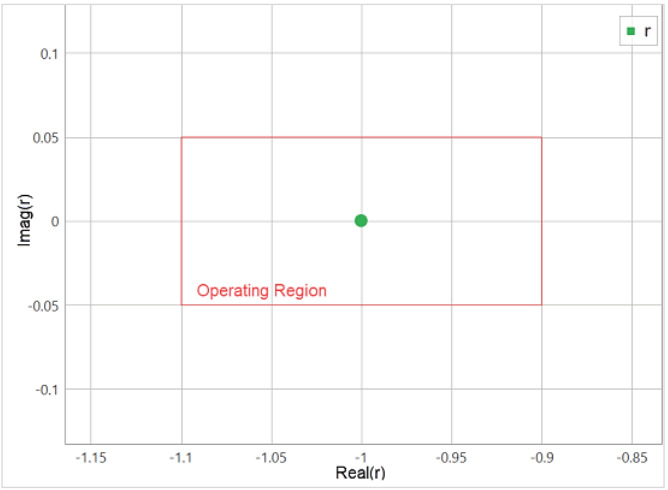

Fig. 2 A complex plane representing the operating region and an ideal operating point for the ratio (r) in the KCL BCD method.

The limitation of the KCL method is that it is inherently non-directional and its operating boundary, both forward and reverse, is restricted based on the amount of load tapped between the relay terminal and the break location. Small amounts of tapped load relative to broken conductor line loading will restrain an element operation. In addition, sources of infeed at buses between the relay and a broken conductor will also tend to restrain the KCL method. In effect, a tightly networked system topology effectively prevents the KCL method from operating for broken conductors external to the line. However, to maximize security, this method is applied only when the charging current remains below a defined maximum threshold, denoted as I_{CH_KCL} in Fig. 1. The I_{CH_KCL} threshold is applied at 1 percent of the relay nominal current

rating to ensure a dependable overlap of the charging current and KCL BCD methods. This ensures that the KCL method detects close-in conductor breaks, while the charging current method covers the rest of the line, thereby maintaining the overall dependability of the detection system [7].

Fault detector logic is applied to block the operation of both the charging current and KCL BCD methods during system shunt faults. This logic monitors for an increase in positive-sequence current and blocks BCD when an increase is detected, as explained in [2]. Additionally, this logic is applied to detect unbalanced, low-magnitude faults and block BCD.

III. Broken Conductor Field Events

Event analysis was performed for three separate field events where aluminum conductor steel-reinforced (ACSR) conductor or buswork connection breaks occurred, all within a year and resulting from common power system equipment failures. In these events, each of the traditional protection systems was reviewed to understand any existing dependability gaps and system reliability concerns. In all applications, BCD was not applied; however, the events were analyzed to understand the expected response of the charging current and KCL broken conductor methods. After describing the expected BCD response, we demonstrate how BCD would have improved the overall dependability of the protection system and reliability of the power system during these events.

A. Broken Conductor on 115 kV Line

A 15.6-mile, 115 kV transmission line interconnects Substation A to Substation B, as represented in Fig. 3. This is a two-terminal transmission line without load taps. The Substation A terminal is equipped with a dual breaker bus arrangement, not shown in Fig. 3 for simplicity. The line protection at each terminal included a directional comparison unblocking (DCUB) pilot scheme coupled with step distance and directional ground time-overcurrent (51G) elements for local backup protection. Additionally, a direct transfer trip (DTT) scheme is applied to transfer trips to remote terminals upon breaker failure. The pilot and direct trip schemes use power line carrier (PLC) signals coupled to the A-phase line conductor.

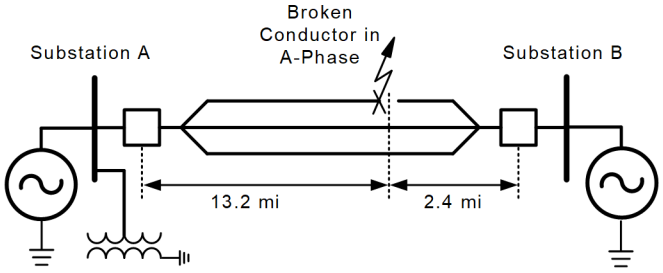

Fig. 3 Broken conductor and shunt fault location on the 115 kV line.

On the night of August 10, 2024, the 115 kV line A-phase conductor broke 13.2 miles from Substation A due to a splice failure (pictured in Fig. 4), resulting in a conductor left hanging and energized from the transmission tower. The small magnitude of the A-phase current is indicative of this conductor break as represented in the Broken Conductor portion of the event recordings in Fig. 5 and Fig. 6.

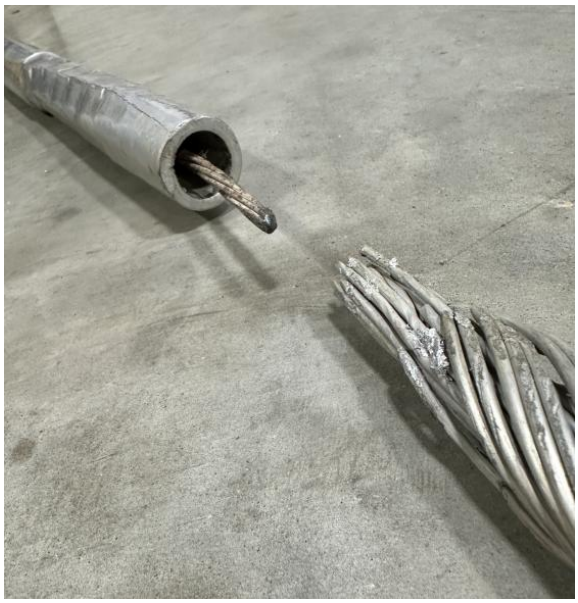

Fig. 4 Splice failure of the 115 kV line.

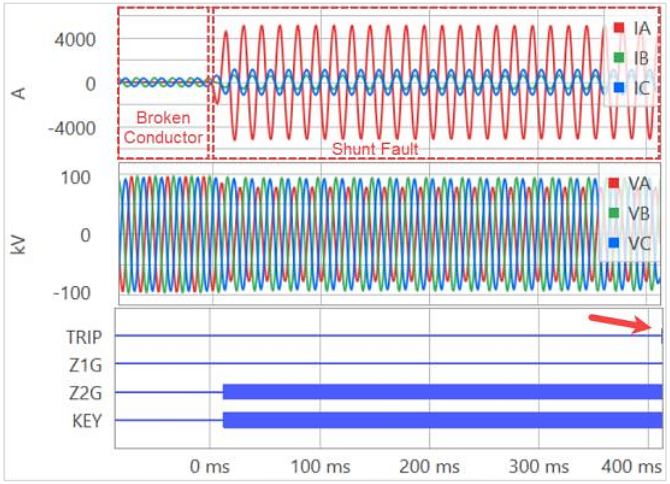

Fig. 5 Relay recording at Substation A of 115 kV line broken conductor and shunt fault event.

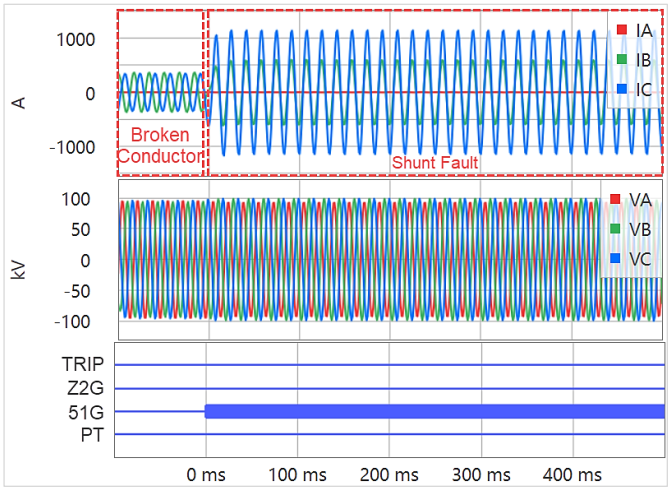

Fig. 6 Relay recording at Substation B of 115 kV line broken conductor and shunt fault event.

Based on the PLC channel loss-of-guard information, it was determined that 590 ms after the conductor broke, the Substation A side of the break contacted the ground, resulting in a line-to-ground (LG) shunt fault. The Substation A relay Zone 2 ground (Z2G) element subsequently detected the fault and transmitted a key signal to the Substation B relay, represented as Z2G and KEY, respectively, in Fig. 5. The permissive trip (PT) signal in the DCUB scheme asserted for 117 ms because the conductor break occurred on the PLC-coupled conductor. This PT signal was the result of the new loss-of-guard condition that started at the inception of the broken conductor. However, the loss-of-guard PT time expired well before the event evolved to include a shunt fault. The deasserted PT signal during the shunt fault state can be observed by the deasserted PT binary element throughout the Substation B recordings from Fig. 6. Thus, a pilot tripping operation never occurred. The Substation A local relay protection tripped in 400 ms on the Z2G delayed trip, as seen in Fig. 5.

After the 115 kV line relay operation at Substation A, the CB3 breaker, shown in Fig. 7, subsequently opened. However, the CB2 breaker was slow to operate (1.05 s), resulting in a breaker failure operation. Therefore, 200 ms after the Substation A relay TRIP binary element asserted, the local CB1 breaker and transformer low-side breaker at Substation C opened. A breaker failure DTT signal was additionally transmitted on the faulted line; however, because the PLC-coupled conductor was broken, the signal was never received at Substation B, so the Substation B breakers did not operate to isolate the event. The final configuration of the system after the breaker failure operation is represented by the breaker statuses in Fig. 7. Notice the slow breaker and failed DTT signal resulted in the positive-sequence source still being available to contribute to the fault on the opposite side of the break through the Substation C ground source via the two unbroken phases.

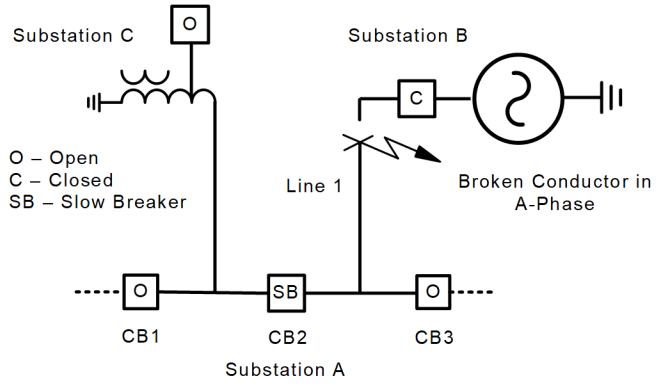

Fig. 7 Simplified one-line diagram of Substation A.

The Substation B contribution to the shunt fault was through remote transformer ground sources. This resulted in a fault apparent impedance well outside the reach of the ground distance elements. The sensitively set directional 51G element asserted shortly after fault inception, as indicated by 51G in Fig. 6. This element, however, never timed out to trip Substation B. With consistent shunt fault current levels, the element would have taken an estimated 700 ms to operate. The transformer ground sources at Substation A were isolated from the fault when the CB1 breaker operated, resulting in the Substation B directional 51G element deasserting, as represented by B:51G in Fig. 8. The CB1 breaker operated 658 ms after the shunt fault inception, just shy of the time required to operate the directional 51G element at Substation B. The CB1 operation to isolate the ground sources local to Substation A from the fault is represented in Fig. 8, where the reduction in current is observed.

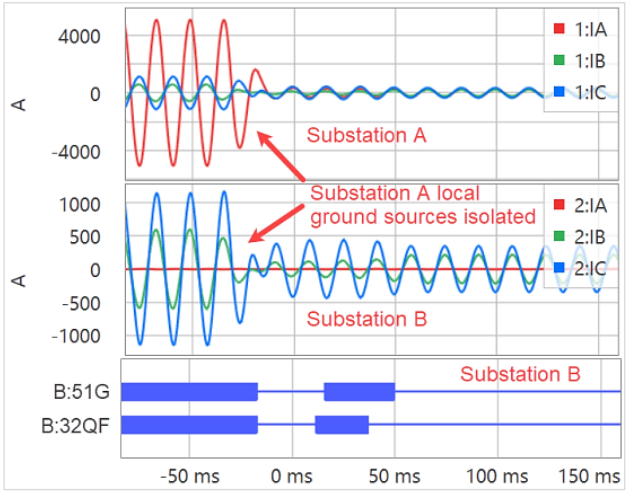

Fig. 8 Fault contribution after breaker fail protection isolates adjacent sources and Substation B is left feeding the fault.

In the Substation B relay, the directional elements were set to give the negative-sequence voltage-polarized directional (32Q) element priority over the zero-sequence voltage-polarized directional (32V) element for 51G directional supervision. The 32Q element correctly declared a forward fault direction when the sources were intact at Substation A. However, after the Substation A sources were isolated, the negative-sequence current reduced below the forward fault detector (50QF) but above the reverse fault detector (50QR) in the 32Q element. This resulted in directional logic giving prioritization to 32Q, but rendering it unable to declare forward, resulting in the deassertion of the directional 51G element. Had 32V been used instead, the directional 51G element could have been made more sensitive and dependable for this event. However, using 32V introduces other challenges including mutual coupling impacts, further explained in [8].

Even if the directional 51G element at Substation B had successfully detected the shunt fault by utilizing 32V directional supervision, it would have taken up to 10 s to trip with CB2 permanently failed. While analyzing the next event, we discuss how to validate ground overcurrent elements for adequate sensitivity and security in conditions where the relay is solely contributing to a shunt fault on its line through a transformer ground source.

The Substation A CB2 breaker eventually opened to isolate the Substation B contribution to the fault 1.05 s after the relay operation at Substation A. Had this breaker not operated, the damage to the fault location and other equipment could have been more severe. After the CB2 breaker isolated Substation B from the shunt fault, the Substation B side of the break was left

energized and hanging from the transmission tower until linemen found it nearly 2 hours later.

Utilization of BCD in the protection scheme would have mitigated several of the concerns from this event. BCD protection locally trips both terminals of a two-terminal transmission line in just tens of milliseconds, preventing the shunt fault from occurring, all while remaining secure. Since BCD isolates the line at both terminals, the safety concern of the hanging conductor would have been mitigated.

Because BCD isolates the event before a shunt fault occurs, the concerns associated with delayed tripping resulting from a lost pilot protection scheme are mitigated. This is particularly important for DCUB schemes which use PLC communications and require a permissive signal or recent loss-of-guard signal to qualify operation. Additionally, isolating the event during the series fault state helps mitigate ground fault sensitivity concerns in the Substation B relaying when the sole shunt fault contribution is through a remote transformer ground source.

A series fault event does not impose substantial stress on the transmission lines and transformers, so it is generally not necessary to initiate a breaker failure scheme when a transmission breaker is called on to operate for a series fault event. As an alternative, protection engineers can apply an additional series fault breaker failure scheme in parallel with the traditional shunt fault breaker failure scheme or, instead, choose not to initiate a breaker failure timer for a series fault relay operation. A series fault breaker failure scheme can be applied with a long breaker failure time delay, up to several seconds, to balance isolating an energized broken conductor to remove a public safety hazard with keeping the system intact for slow breakers.

In this event, if BCD protection elements had been applied without initiating a breaker failure, the CB2 breaker trip would have been initiated in the series fault state and the breaker would have opened prior to timeout of the shunt fault breaker failure scheme. Thus, with BCD protection applied, a shunt fault breaker failure operation would have been prevented. It can be concluded, using BCD protection elements without BCD breaker failure scheme initiation or a parallel series fault breaker failure scheme with an extended delay decreases the chances of a breaker failure scheme operation.

To summarize, BCD provides many benefits beyond overall equipment and system stress reduction and wildfire mitigation. In addition, BCD can be used to minimize or eliminate several concerns presented in this event, including:

- Substation B local protection was unable to isolate its terminal, leaving an energized conductor hanging from the transmission tower.
- Substation A traditional relay protection was delayed in operating because the PLC path was severed.
- A slow operating breaker causing a breaker failure scheme operation resulted in a more impactful outage.

Using the event report data, we looked at the performance of the KCL BCD method. The total charging current on the 115 kV line was below the post-break charging current threshold, I_{CH_CC}, as discussed in Section II. Therefore, the KCL BCD method was expected to respond to events throughout the length of the 115 kV line. We performed an analysis of the KCL BCD method, outlined in [2], of the recordings from this broken conductor event (with results shown in Fig. 9 and Fig. 10). The red rectangle in each figure represents the boundaries of the operating region of the KCL BCD method. The green lines represent the operating locations of the ratio (r), defined by (1) in Section II, during the broken conductor condition. The operating point of the ratio remains well within the operating region during these event captures, indicating the KCL BCD method would have easily detected this event.

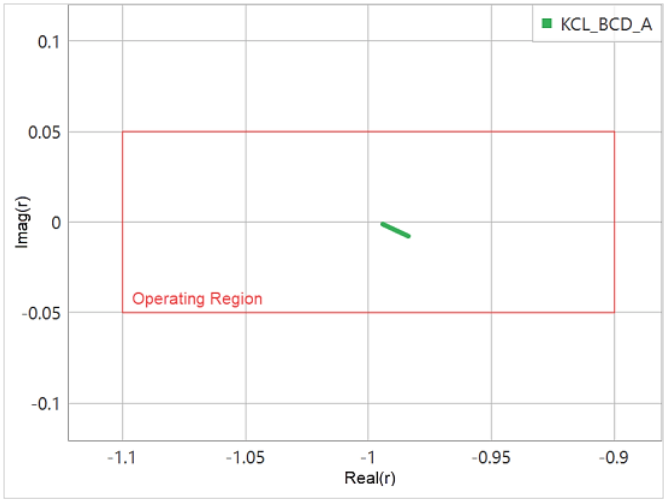

Fig. 9 KCL BCD analysis of Substation A recording from Broken Conductor area of Fig. 5.

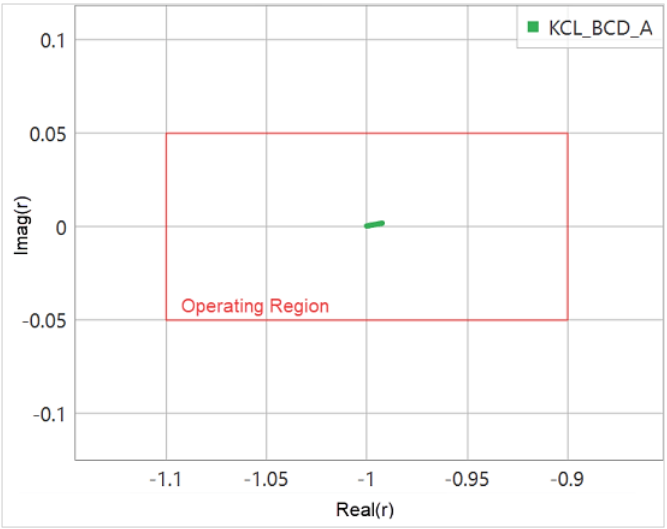

Fig. 10 KCL BCD analysis of Substation B recording from Broken Conductor area of Fig. 6.

B. Broken Buswork at 345 kV Substation B

A 21.4-mile, 345 kV transmission line interconnects Substation A to Substation B, as shown in Fig. 11. This is a two-terminal transmission line without load taps. At Substation B, the 345 kV line directly terminates into a 345 kV to 230 kV autotransformer. The protection scheme at each terminal includes dual-piloted DCUB and permissive overreaching transfer trip (POTT) schemes coupled with step distance and directional 51G elements applied for local backup

tripping. A DTT scheme is applied for transferring trips to remote terminals upon breaker failure. Additionally, because the transformer does not have a high-side breaker, the transformer protection shares a DTT signal to remote-trip the Substation A terminal upon a transformer protection operation. The pilot schemes use both PLC signals coupled to the B-phase line conductor and a leased four-wire audio tone circuit. The Substation B line relay current transformers (CTs) were applied on the transformer high-side bushings and the capacitor voltage transformer (CVT) on the line side of this broken conductor, as represented in Fig. 12.

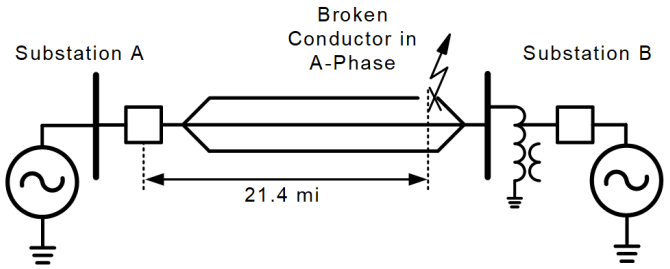

Fig. 11 Broken conductor and shunt fault location on the 345 kV line.

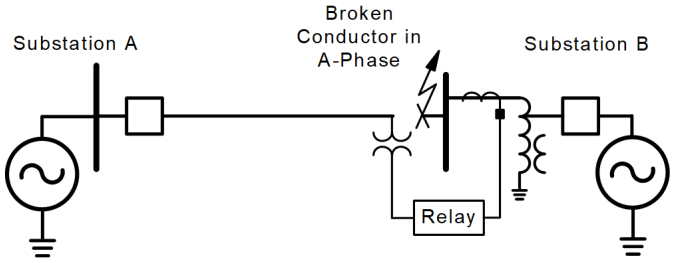

Fig. 12 One-line diagram showing CT and CVT placement with respect to the conductor break.

On the morning of April 28, 2024, during a storm with strong, straight-line winds, the A-phase bus insulator at Substation B broke, resulting in a broken bus and line jumper connection, as seen in Fig. 13. The lack of measurable A-phase current in the Broken Conductor area of Fig. 14 suggested a break in the transmission path. Additionally, the broken conductor can be observed in the Substation A digital fault recorder (DFR) recordings in Fig. 15 by the presence of smaller amounts of current. In this event, the A-phase current had a 90-degree leading phase angle relationship with respect to the A-phase voltage. These characteristics suggest the measured current predominantly results from line-charging capacitance on the A-phase conductor, a condition we would expect during an A-phase broken conductor.

The Substation B side of the break contacted ground 817 ms after the conductor break, resulting in an LG fault as observed in the beginning of the Shunt Fault area of Fig. 14. The Substation B line relaying subsequently operated via an instantaneous directional ground overcurrent element, noted as 67G1 in Fig. 14, resulting in the operation of the transformer low-side breakers. Because the CVTs were isolated from the fault through the conductor break, relay voltages changed very little in this event, resulting in no operation of the ground distance elements at Substation B. This highlights a benefit of instantaneous ground overcurrent elements in line protection schemes when VTs are applied on the line side of the line breakers. Additionally, the pilot protection did not include directional ground overcurrent elements; therefore, a key signal, noted as KEY in Fig. 14, was not transmitted to the Substation A relaying.

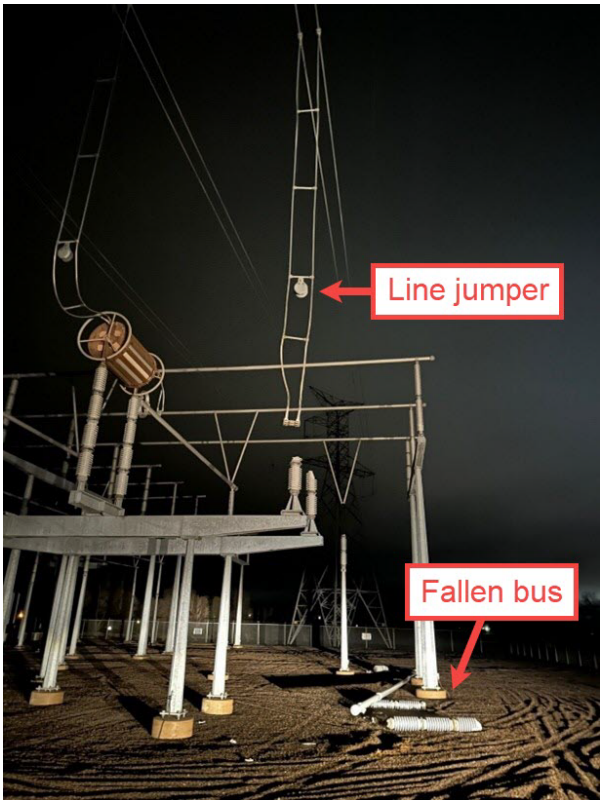

Fig. 13 Broken conductor and shunt fault location on the 345 kV line.

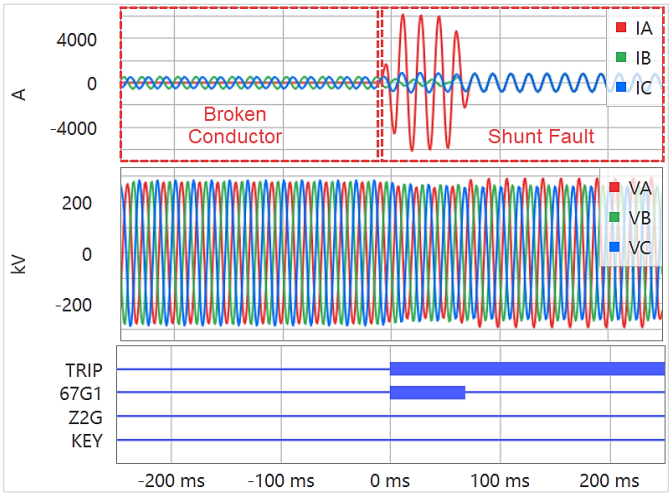

Fig. 14 Relay recording at Substation B of 345 kV line broken conductor and shunt fault event.

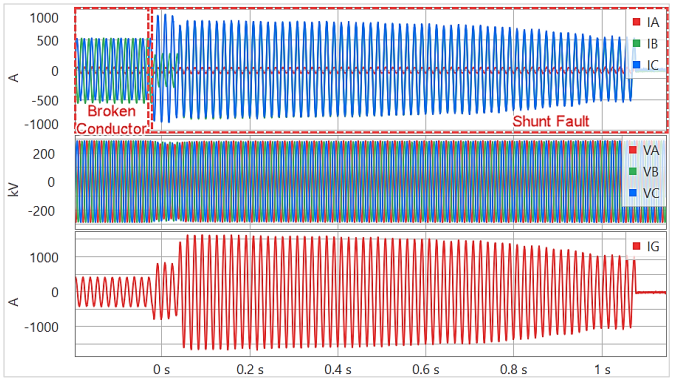

Fig. 15 DFR recording at Substation A of 345 kV line broken conductor and shunt fault event.

The Substation A fault contribution was solely through the Substation B passive autotransformer ground source because the location of the fault was on the transformer side of the break, as represented in Fig. 11. This contribution can be seen in the Shunt Fault area of the Substation A DFR recordings in Fig. 15. Due to an infeed condition at the Substation B transformers, the ground current measurement at the beginning of the shunt fault in the Substation A recordings resulted in lower zero-sequence current measurements as compared to after the infeed sources were removed 59 ms into the shunt fault. The apparent impedance from this contribution, even after Substation B tripped to remove infeed, was large enough that the ground distance elements in the pilot scheme failed to assert, resulting in no operation of the pilot scheme. The pilot scheme did not include directional ground overcurrent elements. After 1.09 s, the neutral time-overcurrent protection tripped on the Substation B autotransformers and keyed a DTT signal to Substation A, tripping the Substation A breakers to isolate the fault. During this time, the Substation A local directional 51G element was picked up but had not yet timed out to trip.

The electrical connection to the shunt fault for Substation A was through the Substation B transformer ground source. Therefore, because this event occurred close-in to Substation B, it provided a best-case scenario for Substation A to dependably detect a simultaneous broken conductor with an LG fault on the transformer side of the break. If the fault location were physically closer to the Substation A terminal, the fault would move further electrically from both the Substation A and B terminals. For this fault type, the fault location requiring the most sensitivity to dependably detect the shunt fault was close-in to the Substation A terminal.

This event highlights the usefulness of directional ground overcurrent elements in both the local and pilot tripping schemes. These elements increase the protection scheme sensitivity to detect ground faults with a high apparent impedance on the protected line, such as the shunt fault in this event. The broken conductor condition coupled with a shunt fault on a single side of the break excites both the negative- and zero-sequence networks on the Substation A side of the break. However, the zero-sequence network had a stronger response during the event. To maximize the sensitivity and dependability of directional ground overcurrent elements for this condition, the settings engineer should carefully consider the overcurrent and directional settings. As was learned from the 115 kV event, ensuring the 32V directional element is allowed to operate provides the best directional element sensitivity and dependability when the terminal's sole contribution to a fault is through a pure zero-sequence transformer ground source. This is further explained in [8].

To do this, the ground overcurrent element pickup and the 32V fault detector settings need to be carefully considered to maintain dependability of 32V. To ensure ground overcurrent elements remain dependable during this condition, the element pickup settings and 32V forward fault detector (50GF) must be set below the $3I_{0L}$ calculated from (2) with a dependability factor. $3I_{0L}$ in (2) provides the lowest expected ground current without infeed at Substation A when a simultaneous conductor break and shunt fault occur close-in to Substation A. For more information and the derivations of this formula, refer to the Appendix.

$$3I_{0L} = \frac{2 \bullet V_S}{\left[\begin{array}{c} 2/3 \bullet Z_{1S} + 4/3 \bullet Z_{0S} + 3 \bullet Z_{0L} \\ + 3 \bullet Z_{0PT} + R_F \end{array}\right]} \quad (2)$$

where:

V_S is the system nominal line-to-neutral voltage

Z_{1S} is the source positive-sequence impedance

Z_{0S} is the source zero-sequence impedance

Z_{0L} is the line zero-sequence impedance

Z_{0PT} is the transformer zero-sequence impedance

R_F is the fault resistance

The directional element impedance threshold settings also need to be carefully considered to maximize the element sensitivity while ensuring security of the element [9]. Because this shunt fault condition often produces small amounts of V0, errors in the V0 measurement can result in a calculated zero-sequence impedance near zero, requiring a positive offset of the forward zero-sequence impedance (Z_{0F}) threshold to dependably detect this shunt fault. A positive offset Z_{0F} threshold introduces other security challenges, such as during an external series fault event, further discussed in [9].

At best, setting ground directional elements to detect this simultaneous conductor break and LG fault is complex. In many applications, it may not be possible to sensitively set ground directional elements to gain 100 percent dependability for this shunt fault event without encroaching on the security limits of the element. Applying BCD simplifies and dependably detects this event in the series fault state, prior to evolution to include a shunt fault. Therefore, with BCD, this event would have been detected, isolated, and the reclosing blocked at each terminal before a shunt fault occurred. Because a shunt fault would never have occurred, the ground sensitivity concerns during a simultaneous series and shunt fault condition are mitigated.

As previously mentioned, one pilot scheme utilized PLC as the communications medium. In this event, the phase conductor coupled with the PLC signal did not break. However, in the 33 percent chance the break occurred on the PLC-coupled conductor, both the pilot and DTT PLC schemes would have been lost. This demonstrates the value of independent channel

communications schemes. As mentioned in the 115 kV line event analysis, BCD can be applied to address the PLC dependability gap during a broken conductor incident.

From the Substation A DFR recording in Fig. 15 and the Substation B relay event recording in Fig. 14, a broken conductor condition can be observed in the area labeled Broken Conductor. The total line-charging current on the 345 kV line is well over the I_{CH_CC} threshold from Fig. 1; therefore, the charging current BCD method is very effective at detecting conductor breaks on this line other than those close-in to the respective relay terminal. Since the break occurred at Substation B, the Substation A relays measured the total line-charging current in this event. Therefore, the charging current measured from this terminal was expected to be well over the I_{CH_KCL} threshold, disabling the KCL BCD scheme. Thus, the charging current BCD scheme was solely expected to respond to detect this event from Substation A.

To demonstrate the response of the charging current BCD scheme outlined in [1], we replayed the Substation A event recording into a relay with the BCD scheme enabled. Fig. 16 demonstrates that the charging current BCD scheme successfully detected this event within 47 ms, as the BCZ2 relay binary element indicates. To maintain selectivity and coordination with adjacent lines, a coordination delay was added to the BCZ2 element resulting in an overall operation time of 265 ms, as observed with the BCDET relay binary element. For three pole tripping applications, this delay is not required with remote terminal loading restraining the element. The observed charging current from this event was 0.079 A secondary, well above the 0.035 A I_{CH_CC} threshold for 5A relay nominal current inputs. Additionally, this playback test located the break at 21.56 miles, only 0.16 miles away from the reported location of the break, demonstrating that the fault locating capabilities of the charging current algorithm help improve line dispatch time when broken conductor events occur.

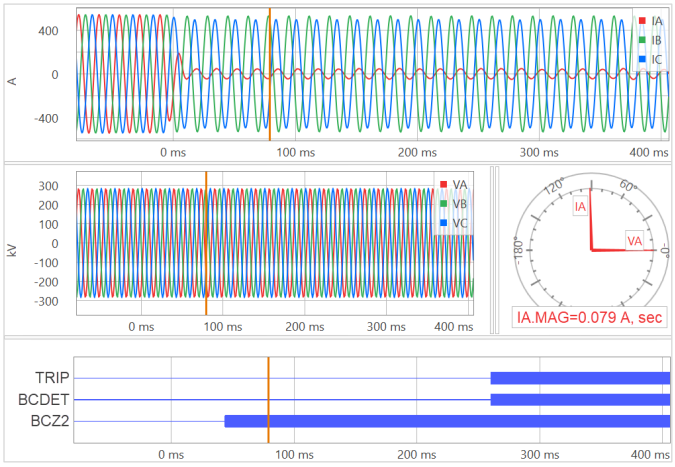

Fig. 16 Charging current BCD results from playback of Substation A.

Using the event report data, we looked at the performance of the KCL BCD method in both terminal relay recordings, with results shown in Fig. 17 and Fig. 18. Because the break was at Substation B, the KCL BCD was expected to solely respond to the event from the Substation B terminal. The red rectangles in the figures represent the boundaries of the operating region of the KCL BCD method. The green lines represent the operating locations of the ratio (r) during the broken conductor condition. The operating point remained well within the operating region during these event captures, indicating that the KCL BCD method, too, would have easily detected this event.

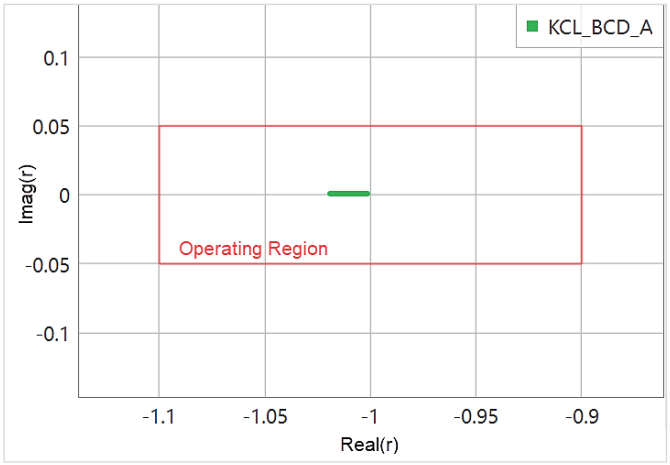

Fig. 17 KCL BCD analysis of Substation A recording from Broken Conductor area of Fig. 15.

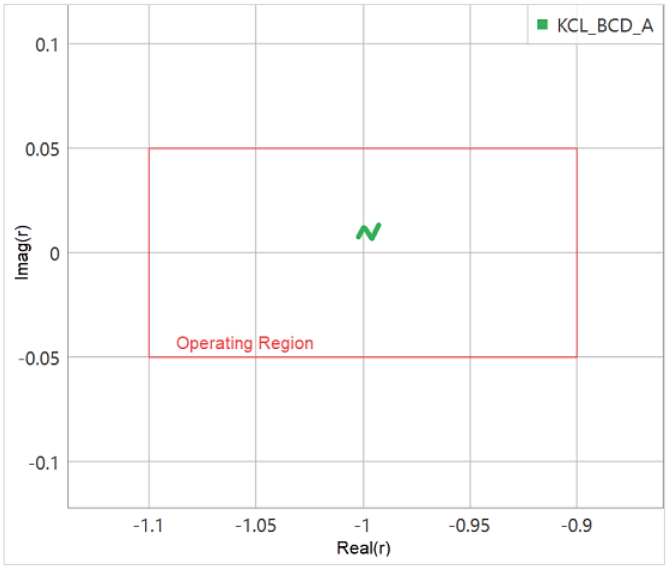

Fig. 18 KCL BCD analysis of Substation B recording from Broken Conductor area of Fig. 14.

C. *Broken Conductor on 161 kV Line*

A 46.46-mile, 161 kV transmission line interconnects Substation A to Substation B, as shown in Fig. 19. This is a two-terminal transmission line without load taps. At Substation B, the 161 kV line directly terminates into a 161 kV to 115 kV autotransformer. The protection scheme at each terminal includes POTT and direct underreaching transfer trip (DUTT) pilot protection schemes. For local backup protection, the schemes also include step distance and directional 51G elements at each terminal. A DTT scheme is applied for transferring trips to remote terminals upon breaker failure. Additionally, because Substation B does not have a high-side

breaker, a DTT scheme is used to remote-trip the Substation A terminal during transformer protection operations at Substation B. The pilot scheme uses multiplexers with a microwave system as the communications path.

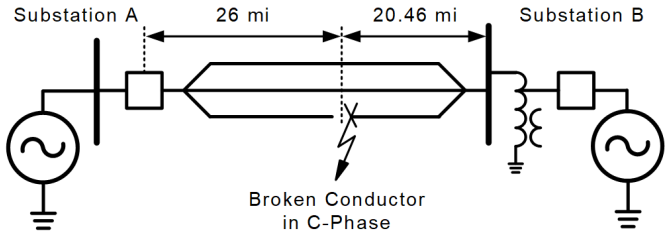

Fig. 19 Broken conductor and shunt fault location on 161 kV line.

On the afternoon of February 20, 2025, a helicopter struck the line conductor, resulting in a broken conductor event 20.46 miles from Substation B, as shown in Fig. 19. Small magnitudes of line-charging current on C-phase at each terminal in the Broken Conductor area of Fig. 20 and Fig. 21 suggest a broken conductor on the transmission line. 665 ms after the conductor break, the Substation B side of the break contacted ground, resulting in an LG fault, as indicated in the Shunt Fault area of Fig. 20 and Fig. 21.

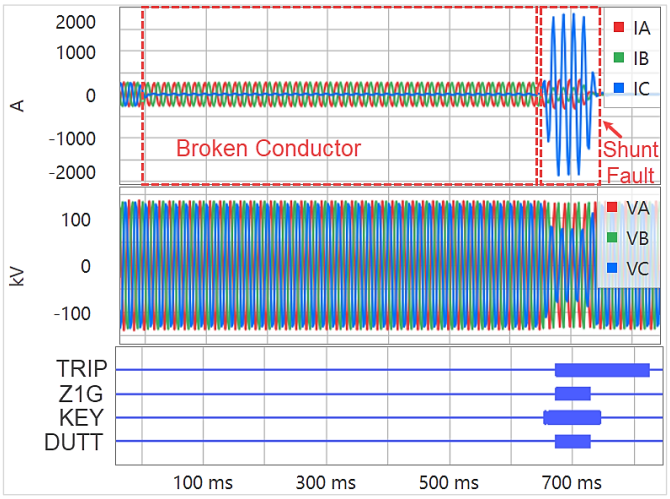

Fig. 20 Relay recording at Substation B of the 161 kV line broken conductor and shunt fault event.

The Substation B line relay operated via the Zone 1 ground (Z1G) distance element, represented by the Z1G relay binary element in Fig. 20, and the transformer low-side breaker subsequently opened. Additionally, the Substation B relaying transmitted both a POTT permissive key and a direct underreaching trip, represented respectively by the KEY and DUTT relay binary elements in Fig. 20.

Like the previous event on the 345 kV line, the Substation A contribution to the fault was through the Substation B autotransformer with infeed at the transformer location. This infeed, coupled with the added transformer and line impedance, creates a high apparent impedance in the Substation A shunt fault path. This is indicated by the small increase in currents from load levels and the negligible change in voltage in the shunt fault area of Fig. 21. This apparent impedance was large enough to prevent the ground protection elements (Z2G and 67G2 in Fig. 21) from asserting at Substation A, resulting in no POTT scheme operation. Substation A tripped after receiving the direct underreaching trip receive signal from Substation B relaying, represented by the DUTR relay binary element in Fig. 21. This event demonstrates the dependability benefits of applying a POTT pilot scheme in parallel with a DUTT pilot scheme in line-connected transformer applications. However, a DUTT scheme is still dependent on functioning communications to successfully trip both terminals and, depending on the communications medium, can be susceptible to security issues resulting from channel noise.

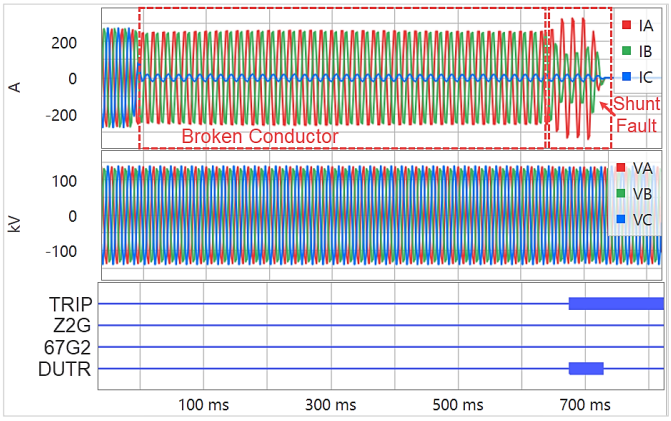

Fig. 21 Relay recording at Substation A of the 161 kV line broken conductor and shunt fault event.

This event is another reminder of how broken conductor events can challenge traditional protection schemes and how BCD improves overall line protection scheme performance. BCD locally trips at both line terminals, resulting in a dependability increase in isolating the event before a shunt fault occurs.

The breakers at both Substation A and Substation B attempted reclosing at different times to restore the line, only to fault and trip after reclose and lockout of the line. During the reclosing open interval, the Substation A side of the broken conductor made contact with ground, generating an LG fault condition on both sides of the conductor break, thereby enabling the local protection elements at Substation A to detect and isolate the shunt fault on reclose with relative ease. Had the Substation A side of the broken conductor not contacted ground, Substation A would have had difficulty locally detecting the shunt fault contribution through the remote terminal transformer ground source. Like previous events, this fault scenario challenges the sensitivity and dependability of the directional 51G element, particularly as the fault location moves closer to Substation A. This event presents a similar electrical response to the earlier 345 kV line event, but the fault location is in the middle of the line making shunt fault protection sensitivity even more important.

As explained earlier, adding BCD elements to the protection scheme helps to mitigate directional 51G sensitivity concerns during this fault scenario because it detects and isolates this fault condition in the series fault state. Additionally, because a broken conductor is a permanent event, when the BCD protection operates, the reclosing function is driven to lockout.

In this event, BCD would have prevented unnecessary reclose attempts, resulting in less equipment stress and improved safety at the incident location.

From the Substation A and B relay event recordings (Fig. 20 and Fig. 21, respectively), a broken conductor condition can be observed in the area labeled Broken Conductor. The total line-charging current on the 161 kV line is over the I_{CH_CC} threshold in Fig. 1; therefore, the charging current BCD method is effective in detecting line breaks on 70 percent of this line from each terminal. The location of the break in this event produced enough charging current at each terminal to allow the charging current BCD method to detect this event. To demonstrate the response of the charging current BCD scheme, we replayed the Substation A and Substation B events into relays with the BCD scheme enabled. The event recordings from the Substation A playback in Fig. 22 demonstrate that the charging current BCD scheme successfully detected this break event within 55 ms and tripped in 105 ms at Substation A, represented by the BCZ1 and BCDET relay binary elements, respectively. The observed charging current from this event was 0.081 A secondary, well above the 0.035 A I_{CH_CC} threshold on 5 A relay nominal current inputs.

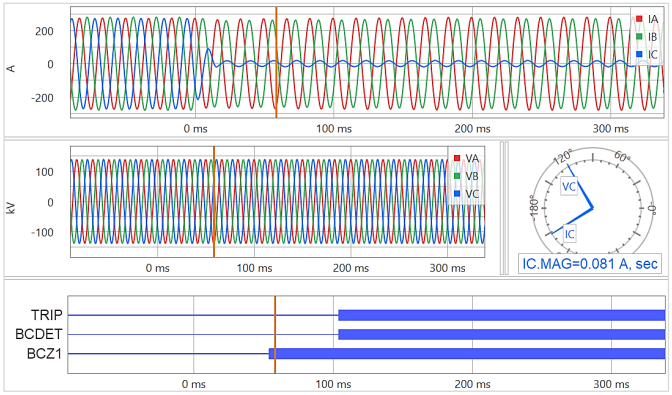

Fig. 22 Charging current BCD results from playback of Substation A.

At Substation B, the charging current BCD scheme successfully detected the event in 48 ms and tripped in 98 ms, represented respectively by the BCZ1 and BCDET relay binary elements in Fig. 23. The observed charging current from this event was 0.04 A secondary, above the 0.035 A I_{CH_CC} threshold on 5 A relay nominal current inputs. Additionally, the broken conductor break location algorithm reported a break 25.31 miles from Substation A and 20.99 miles from Substation B. This resulted in a location accuracy of 0.69 miles from Substation A and 0.53 miles from Substation B, greatly aiding dispatch efforts.

Using the event report data, we looked at the performance of the KCL BCD method in both terminal relay recordings, with results shown in Fig. 24 and Fig. 25. The red rectangles in the figures represent the boundaries of the operating region of the KCL BCD method. The green lines represent the operating locations of the ratio (r) during the broken conductor condition. The operating point remained well within the operating region during the broken conductor state of these event captures, indicating the KCL BCD method, too, would have easily detected this event.

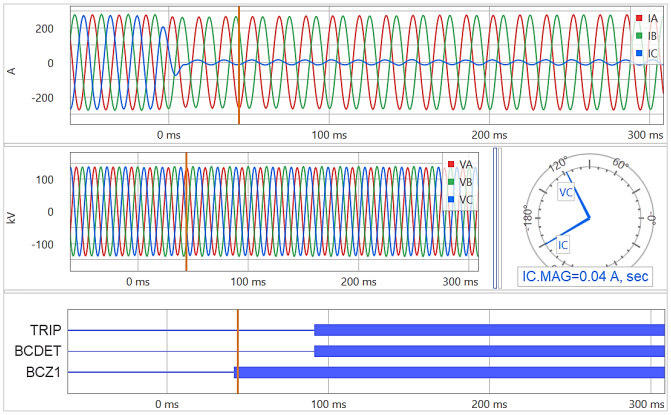

Fig. 23 Charging current BCD results from playback of Substation B.

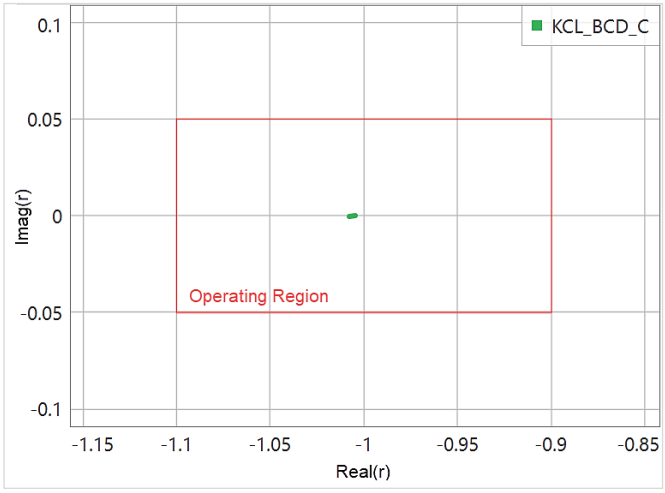

Fig. 24 Charging current BCD playback of Substation A recording from Broken Conductor area of Fig. 21.

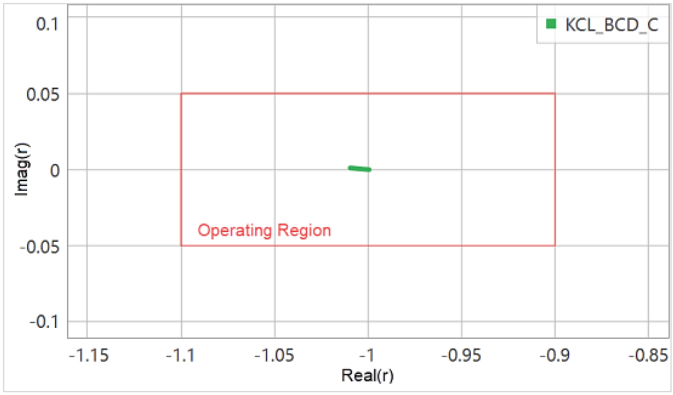

Fig. 25 Charging current BCD playback of Substation B recording from Broken Conductor area of Fig. 20.

IV. Dependability Analysis

The methods described in Section II work well to dependably detect from both terminals a broken conductor on two-terminal transmission circuits without taps. These methods, however, lose dependability in more complicated systems or when a series arc is slow to extinguish. Next, we discuss these limitations and offer solutions to gain back dependability in these applications.

A. *Slower Detection of Broken Conductor Fault*

A mechanical break in a conductor can lead to the formation of a series arc between the separated conductor ends. The duration of series arcing can be substantial, often lasting several hundred milliseconds. The arc eventually extinguishes as the physical separation between the conductor segments increases [3]. Until this occurs, the detection methods in Section II remain inactive, thereby delaying the detection of the broken conductor.

Fig. 26 illustrates a C-phase broken conductor field event where the series arcing causes a reduction in phase current magnitude and a corresponding increase in ground current. This triggers a sensitive ground protection element, resulting in a trip without correctly identifying the event as a broken conductor fault. Upon reclosing, as shown in Fig. 27, the relay trips again, as the conductor has by then fallen to the ground, creating a permanent fault.

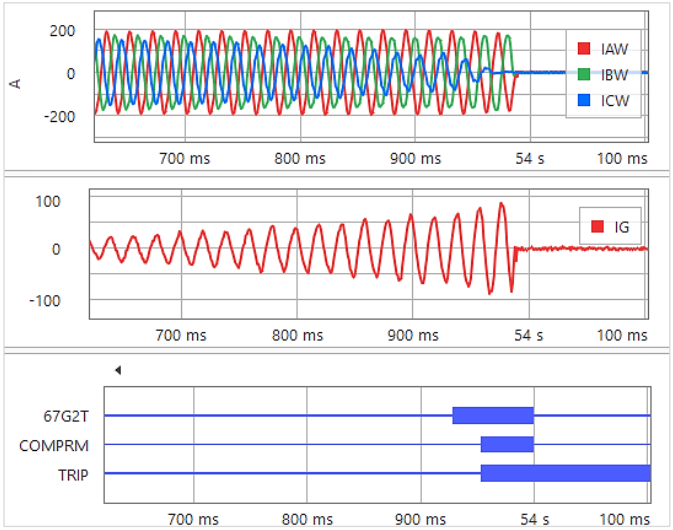

Fig. 26 Field event showing series arcing caused by broken conductor in C-Phase.

In this event, the detection method in Section II failed to identify the broken conductor because the relay operated before the arc was extinguished, leading to a BCD dependability issue. To address such limitations, the techniques described in [3] offer the capability to detect series arcing caused by conductor breaks. These methods can be integrated alongside the approach in Section II to block reclosing, particularly in systems with sensitive negative-sequence or ground current protection elements. This combined strategy enhances the overall reliability and responsiveness of BCD.

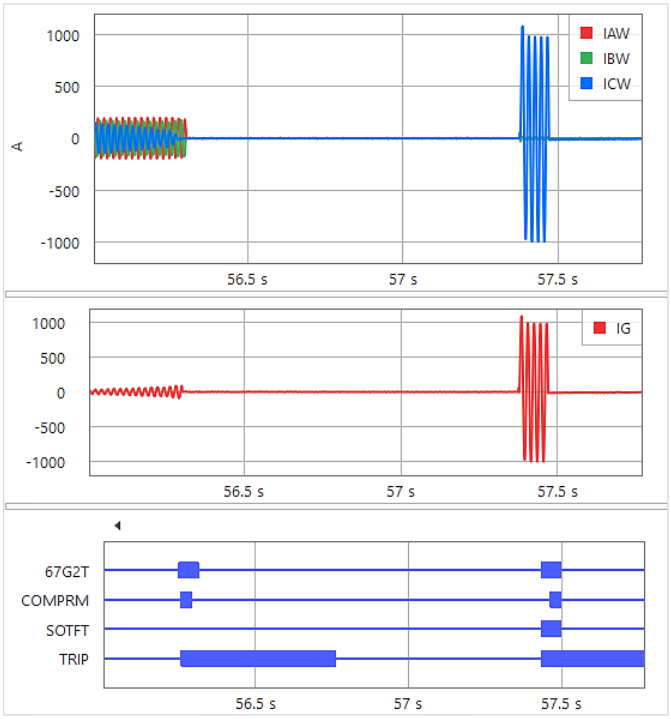

Fig. 27 Event record showing autoreclosing after the broken conductor phase had fallen to the ground.

B. *Broken Conductor Fault Between Taps*

The charging current and KCL BCD methods are effective at identifying conductor breaks along the transmission line segment extending from a relay terminal up to the first tapped load. In a line configuration with only one tap, a broken conductor occurring between the relay terminal and the tap can be detected by the relay at that terminal but not at the opposite terminal. This limitation arises because the relay at the opposite terminal measures not only the line's charging current but also the load current drawn by the tap. As a result, the presence of tap load masks the line-charging current that the charging current detection algorithm relies on, rendering it ineffective. Similarly, the KCL method is compromised in this scenario. The tap load introduces additional positive-sequence current, which lowers the sequence current ratio used in the KCL algorithm, leading to a dependability reduction. Despite these limitations, the system retains its ability to detect broken conductors because at least one terminal (the terminal without tapped load between it and the break) can still identify the fault. Upon detection, this terminal can issue a direct trip signal to the relay at the opposite terminal, ensuring that the BCD scheme remains dependable and the broken conductor condition is addressed promptly.

However, in more complex line configurations with multiple taps, such as the one illustrated in Fig. 28, the BCD capability becomes more constrained. In such cases, the relays at terminal stations (e.g., Station A and Station B) can only detect a broken conductor if it occurs between the terminal and the first tapped load on their respective sides. If the conductor break occurs between two intermediate tapped loads, neither terminal can dependably detect the fault using the existing algorithms described in Section II.

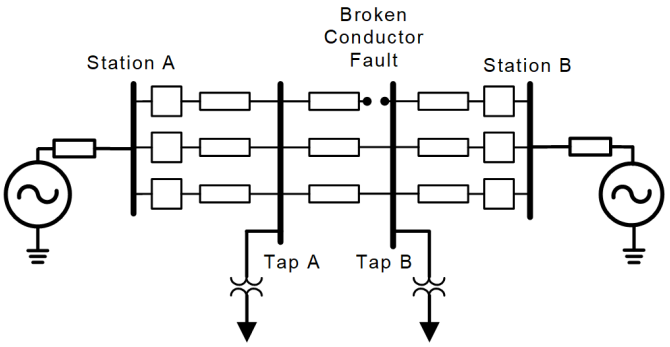

Fig. 28 Broken conductor example on a line with several tapped loads.

To address this dependability gap, an alternative approach is required. One viable solution involves implementing a series arcing detection algorithm, as outlined in [3]. If the conductor break results in series arcing, this algorithm can identify the arcing signature and thereby detect the broken conductor condition even when it occurs between taps, an area otherwise blind to the original detection methods.

V. Improvements

For successful deployment of BCD, the detection algorithms must remain secure. Both the charging current and KCL BCD algorithms are designed to restrain operation when load current measurements are very low and during power system faults, per [1] and [2]. The charging current and KCL BCD methods are inherently secure for many fault conditions. Certain phase-to-phase fault conditions, however, can challenge BCD methods. Therefore, fault detectors are used to block BCD schemes during such faults.

As mentioned earlier, the KCL detection method is a non-directional element without an inherently defined operating boundary. This is why the KCL method is applied in conjunction with the charging current method, and the KCL element operation is blocked when charging current measurements are high enough for the charging current method to detect. Additionally, the KCL method is inherently restrained when load is present between the break and the relay measurement point. Therefore, the KCL method operating boundary is restrained either by I_{CH_KCL} or to the respective substations when small quantities of load are tapped at the local and remote terminals.

VI. Conclusion

Broken conductor conditions can occur for several reasons. In this paper, we provided three examples of events where ACSR conductor breaks occurred because of a failed splice, a fallen bus resulting from straight-line winds, and a helicopter strike. As the events demonstrate, detecting broken conductor events after they evolve to a shunt fault can challenge traditional shunt fault protection schemes, particularly when only one side of the break results in a shunt fault. Some challenges include severed communications paths, fault sensitivity concerns, and reclosing into a permanent fault. BCD protection can improve the performance of protection schemes by complementing traditional protection schemes during broken conductor events. In addition, BCD detection can enhance breaker failure schemes by offering the breaker more time to operate prior to a shunt fault occurring, increasing the possibility that a slow breaker successfully operates before the breaker failure scheme trips.

The enhanced BCD scheme described in this paper uses the charging current and KCL broken conductor methods. These schemes combine to provide dependability to 100 percent of the protected line for broken conductor events using local measurements only. The events discussed demonstrate that these schemes complement one another well. Additionally, the charging current broken conductor location algorithm accurately identifies the break point, enabling faster dispatch response.

The events described within this paper demonstrated how BCD protection improves existing shunt fault protection systems and demonstrated the dependability of the charging current and KCL BCD methods. BCD protection is one of the few line protection or monitoring schemes that successfully detects, trips, and prevents reclosure for a permanent line problem before a shunt fault occurs, mitigating the additional stress a shunt fault places on the power system among other concerns. All of these benefits suggest that, one day, BCD protection could be more commonplace in transmission and subtransmission protection schemes.

VII. Appendix

In applications with line-connected transformer ground sources, it is imperative that settings engineers consider the impact of a simultaneous broken conductor with an LG fault on the transformer side of the break when applying relay settings. As explained earlier, using BCD elements to detect the series fault condition before the fault evolves to include a simultaneous LG fault mitigates the ground sensitivity concerns during this simultaneous series and shunt fault event.

Fig. 29 provides a transmission line example of a power line with a line-connected transformer ground source. In the example, the A-phase conductor is broken a distance, m, in per unit from the Substation A terminal and a simultaneous A-phase to ground (A–G) fault occurs directly on the transformer side of the break. This example is used to demonstrate how to derive sequence currents to validate the sensitivity of ground overcurrent protection at Substation A.

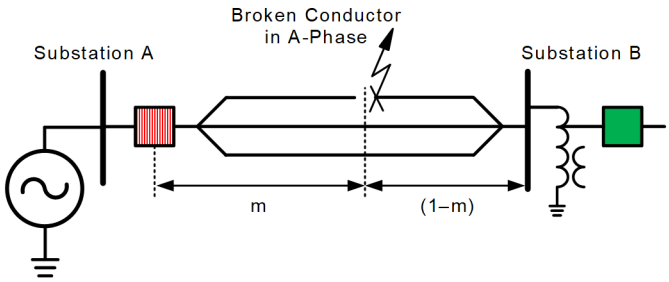

Fig. 29 A-phase broken conductor with simultaneous A–G fault on a system with line-connected transformer ground source.

If ground elements are used to detect this simultaneous fault, high sensitivity in ground protection elements is required. This

sensitivity impacts both pilot schemes and local tripping schemes alike. The following discussion produces a formula to calculate the lowest expected I_{0L} current for this simultaneous fault condition. As previously explained, the scenario requiring the highest sensitivity in ground protection elements is a break close-in to the Substation A terminal with the LG fault applied on the transformer side of the break, as represented in Fig. 29, where m = 0. In this example, we assume the broken conductor and LG fault both occur in A-phase. The sequence network for this simultaneous fault condition is represented in Fig. 30, with the autotransformer represented using a T model. An ideal transformer with a ratio of 1:1 is placed across the break in all the sequence networks [10] [11]. As a result, all the sequence voltages across the break are equal, and represented as V_{xy} in Fig. 30. The Substation A and Substation B relay sequence currents are denoted with L and R in the subscript, respectively.

In this example, the local A-phase current must be equal to zero. Therefore:

$$I_{AL} = I_{1L} + I_{2L} + I_{0L} = 0 \tag{3}$$

Because I_{1L} and I_{2L} are equivalent in Fig. 30, (3) can be rearranged to reveal the following relationships:

$$2 \bullet I_{1L} = 2 \bullet I_{2L} = -I_{0L} \tag{4}$$

Additionally, KCL can be applied at node N and rearranged to reveal:

$$I_{0R} = I_{1L} - I_{0L} \tag{5}$$

Using the current relationships in (4) to rewrite (5) reveals:

$$I_{0R} = 3 \bullet I_{1L} = 3 \bullet I_{2L} \tag{6}$$

Kirchhoff's voltage law can then be applied around the red dash current (Loop 1) and green half-dash current (Loop 2) to reveal (7) and (8), respectively. The current relationships from (4) and (6) are then used to rearrange equations (7) and (8) to reveal (9) and (10) for Loops 1 and 2, respectively, assuming Z_{1S} and Z_{2S} are equivalent, as are Z_{1L} and Z_{2L}. Z_{0PT} ($Z_{0Tp} + Z_{0Tt}$) represents the transformer zero-sequence impedance from the primary to tertiary winding.

$$\begin{aligned} V_S = {} & I_{1L} \bullet (Z_{1S} + m \bullet Z_{1L} + 3 \bullet R_F) \\ & + I_{2L} \bullet (Z_{2S} + m \bullet Z_{2L}) \\ & + I_{0R} \bullet (Z_{0PT} + (1 - m) \bullet Z_{0L}) \\ & + 2 \bullet V_{xy} \end{aligned} \tag{7}$$

$$\begin{aligned} V_{xy} = {} & I_{0R} \bullet (Z_{0PT} + (1 - m) \bullet Z_{0L}) \\ & - I_{0L} \bullet (Z_{0S} + m \bullet Z_{0L}) \end{aligned} \tag{8}$$

$$\begin{aligned} V_S = {} & I_{1L} \bullet (2 \bullet Z_{1S} + 2m \bullet Z_{1L} + 3 \bullet (1 - m) \bullet Z_{0L} \\ & + 3 \bullet Z_{0PT} + 3 \bullet R_F) + 2 \bullet V_{xy} \end{aligned} \tag{9}$$

$$\begin{aligned} V_{xy} = {} & I_{1L} \bullet (2 \bullet Z_{0S} + 2m \bullet Z_{0L} + 3 \bullet (1 - m) \bullet Z_{0L} \\ & + 3 \bullet Z_{0PT}) \end{aligned} \tag{10}$$

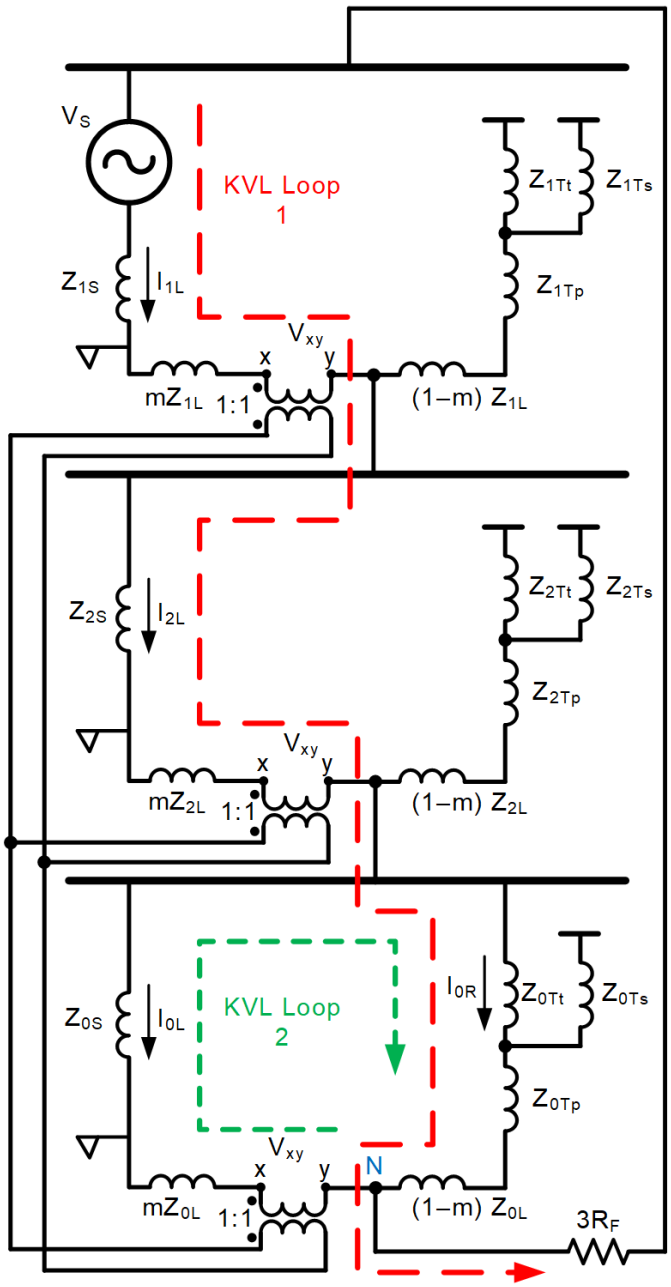

Fig. 30 Sequence diagram for a simultaneous A-phase broken conductor with an A–G fault on the transformer side of the break.

Replacing V_{xy} in (9) with (10) reveals:

$$\begin{aligned} V_S = {} & I_{1L} \bullet (2 \bullet Z_{1S} + 4 \bullet Z_{0S} + 2m \bullet Z_{1L} \\ & + 4m \bullet Z_{0L} + 9 \bullet (1 - m) \bullet Z_{0L} \\ & + 9 \bullet Z_{0PT} + 3 \bullet R_F) \end{aligned} \tag{11}$$

Rearranging (11) to solve for I_{1L} reveals:

$$I_{1L} = \frac{V_S}{\left(\begin{array}{l} 2 \bullet Z_{1S} + 4 \bullet Z_{0S} + 2m \bullet Z_{1L} \\ + (9 - 5m) \bullet Z_{0L} + 9 \bullet Z_{0PT} + 3 \bullet R_F \end{array}\right)} \tag{12}$$

Using the current relationships in (4) and replacing I_{1L} with I_{0L} in (12) reveals:

$$I_{0L} = \frac{-2 \bullet V_S}{\begin{pmatrix} 2 \bullet Z_{1S} + 4 \bullet Z_{0S} + 2m \bullet Z_{1L} \\ + (9 - 5m) \bullet Z_{0L} + 9 \bullet Z_{0PT} + 3 \bullet R_F \end{pmatrix}} \quad (13)$$

Assuming a fault location of m = 0, (13) simplifies to:

$$I_{0L} = \frac{-2 \bullet V_S}{\begin{pmatrix} 2 \bullet Z_{1S} + 4 \bullet Z_{0S} + 9 \bullet Z_{0L} + 9 \bullet Z_{0PT} \\ +3 \bullet R_F \end{pmatrix}} \quad (14)$$

VIII. References

[1] K. Dase, S. Harmukh, and A. Chatterjee, "Detecting and Locating Broken Conductor Faults on High-Voltage Lines to Prevent Autoreclosing Onto Permanent Faults," 46th Annual Western Protective Relay Conference, Spokane, Washington, October 21–24, 2019.

[2] Y. Gong, G. Juvekar, and K. Dase, "Zero-Setting Broken Conductor Detection Method Using Local Measurements Only," proceedings of the 50th Annual Western Protective Relay Conference, Spokane, Washington, October 2023.

[3] K. Dase, J. Colwell, and S. Pai, "Novel Methods for Detecting Conductor Breaks in Power Lines," 76th Annual Conference for Protective Relay Engineers, College Station, Texas, March 2023.

[4] Y. Yin, H. Bayat, N. Dunn M. Leyba, M. Webster, A. Marquez, K. Tran, and A. Torres, "High-Speed Falling Conductor Protection for Electric Power Transmission Systems," 49th Annual Western Protective Relay Conference, Spokane, Washington, October 11–15, 2022.

[5] S. K. Lau and S. K. Ho, "Open-Circuit Fault Detection in Distribution Overhead Power Supply Network," Journal of International Council on Electrical Engineering, 7:1, 2017, pp. 269–275.

[6] W. O'Brien, E. Udren, K. Garg, D. Haes, and B. Sridharan, "Catching Falling Conductors in Midair—Detecting and Tripping Broken Distribution Circuit Conductors at Protection Speeds," 42nd Annual Western Protective Relay Conference, Spokane, Washington, October 20–22, 2015.

[7] SEL-411L Instruction Manual. Available: selinc.com

[8] R. McDaniel and Y. Shah, "Improving Ground Fault Sensitivity for Transmission Lines Near Inverter-Based Resources," proceedings of the 50th Annual Western Protective Relay Conference, Spokane, Washington, October 2023.

[9] R. McDaniel and M. Thompson, "Impedance-Based Directional Elements—Why Have a Threshold Setting?," proceedings of the 48th Annual Western Protective Relay Conference, Spokane, Washington, October 2021.

[10] G. Benmouyal and B. Smyth, "Accurate Fault Locating During a Pole-Open Condition," proceedings of the 19th Georgia Tech Fault and Disturbance Conference, Atlanta, Georgia, April 2016.

[11] E.L. Harder, "Sequence Network Connections," Westinghouse Electric and Manufacturing Company.

IX. Biographies

Joe Livingston received his BS in electrical engineering from North Dakota State University in 1993. After graduation, Joe worked at Minnesota Power, where he had previously interned, as a planning engineer and then as a relay engineer. He joined Great River Energy (GRE) in 1997 as a transmission planning engineer and quickly transitioned to a substation design engineer. He is presently a principal engineer responsible for protection system standards and maintenance. In this role, he primarily conducts protection system post-event analysis and ensures company compliance with various North American Electric Reliability Corporation (NERC) standards. Joe is the chairperson of the North American Transmission Forum (NATF) System Protection Practice group and an active contributor sharing knowledge of protection system operations and fault analysis. Joe is a registered professional engineer in the state of Minnesota.

Stephen Marx received his BSEE from the University of Utah in 1988. He joined Bonneville Power Administration (BPA) in 1988 where he is presently the district engineer in Idaho Falls, Idaho. He has more than 37 years of experience in power system protection and metering and has been a lecturer at the Hands-On Relay School in the state of Washington since 2007. He has authored and coauthored several technical papers. He is a registered professional engineer in the state of Oregon and a member of IEEE.

Josh LaBlanc received his BS in electrical engineering from the University of North Dakota in 2011. After graduation, Josh worked for an oil and gas pipeline company, Enbridge Energy, then an electric power utility, Minnesota Power. Josh has most recently spent 6.5 years working as an application engineer for Schweitzer Engineering Laboratories, Inc. (SEL). His primary roles are providing application and technical support and training on power system protection topics. Josh is a registered professional engineer in the state of Minnesota.

Yanfeng Gong earned his BS in electrical engineering with a focus on power systems from Wuhan University, China, in 1998. He then went on to obtain his MSEE from Michigan Technological University in 2002 and his PhD from Mississippi State University in 2005, continuing his specialization in power systems. Yanfeng worked as a research engineer at Schweitzer Engineering Laboratories, Inc. (SEL) from 2005 to 2013. He served as a principal engineer and supervisor at American Electric Power (AEP) in the Advanced Transmission Studies & Technologies (ATST) department from 2013 to 2019. In 2019, he returned to SEL, assuming the role of principal engineer. In addition to his professional endeavors, Yanfeng has played an active role in industry committees. He served as the past chair of the IEEE Transient Analysis and Simulation Subcommittee (TASS) and is currently the vice chair of the IEEE Analytic Methods for Power Systems (AMPS) technical committee. He has been an active contributor to several industry standardization efforts and technical working groups. Yanfeng is a senior member of IEEE and a registered professional engineer (PE) in the state of Washington.

Jordan Bell received his BSEE from Washington State University in 2006. He joined Schweitzer Engineering Laboratories, Inc. (SEL) in 2008 as a protection engineer in the SEL Engineering Services, Inc. (SEL ES) group. He is currently a senior engineer and supervisor in that group, working on event report analysis, relay settings and relay coordination, fault studies, and model power system testing with a real-time digital simulator. He is a registered professional engineer in the state of Washington and a member of IEEE.

Kanchanrao Dase earned his Bachelor of Engineering degree in Electrical Engineering from Sardar Patel College of Engineering, University of Mumbai, India in 2009. He completed his Master of Science degree in Electrical Engineering from Michigan Technological University in 2015. From 2009 to 2014, he worked as a manager at Reliance Infrastructure Limited, with a substation engineering and commissioning profile. He is currently a senior engineer in the Research & Development division at Schweitzer Engineering Laboratories, Inc. (SEL). His interests include power system protection, substation automation, and fault locating. He is a senior IEEE member and a registered Professional Engineer (PE) in Washington State. He has authored several technical papers and currently holds six patents.